Molecular models and activation energies for bonding rearrangement in plasma-deposited a-SiN_x:H dielectric thin films treated by rapid thermal annealing

F. L. Martínez, A. del Prado, I. Mártil, and G. González-Diaz
Departamento de Física Aplicada III, Universidad Complutense de Madrid, E-28040 Madrid, Spain

W. Bohne, W. Fuhs, J. Röhrich, B. Selle and I. Sieber
Hahn-Meitner-Institut Berlin, Glienicker Strasse 100, D-14109 Berlin, Germany

(Received 29 September 2000; revised manuscript received 24 January 2001; published 6 June 2001)

Hydrogen and nitrogen release processes in amorphous silicon nitride dielectrics have been studied by MeV ion scattering spectrometry in combination with infrared spectroscopy. The outdiffusion of those light constituents was activated by the thermal energy supplied to the samples by rapid thermal annealing treatments. Molecular models of how these reactions proceed have been proposed based on the information obtained from the infrared spectra, and the validity of the models has been tested by an analysis of the activation energy of the desorption processes. For this purpose, the evolution of the hydrogen concentration versus the annealing temperature was fitted to an Arrhenius-type law obtained from a second-order kinetics formulation of the reactions that are described by the proposed structural models. It was found that the low values of the activation energies can be consistently explained by the formation of hydrogen bonding interactions between Si-H or N-H groups and nearby doubly occupied nitrogen orbitals. This electrostatic interaction debilitates the Si-H or N-H bond and favors the release of hydrogen. The detailed mechanism of this process and the temperature range in which it takes place depend on the amount and the proportion of hydrogen in Si-H and N-H bonds. Samples with higher nitrogen content, in which all bonded hydrogen is in the form of N-H bonds, are more stable upon annealing than samples in which both Si-H and N-H bonds are detected. In those nitrogen-rich films only a loss of hydrogen is detected at the highest annealing temperatures.

DOI: 10.1103/PhysRevB.63.245320 PACS number(s): 68.60.Dv, 61.43.Er, 81.40.Tv, 82.20.Pm

I. INTRODUCTION

Amorphous hydrogenated silicon nitride (a-SiN_x:H) is a high-permittivity dielectric whose properties are specially suitable to look into the physics of amorphous solids and into the important role of hydrogen in semiconductors.[1] In particular, its response to thermal treatments is a convenient way of investigating details of the bonding structure and network topology, by means of the lattice reactions that may be started up by thermal activation. Thereby, the hydrogen content in the dielectric, its amount and distribution, plays a key role in determining the special kind of lattice reaction and network rearrangement.[2] In plasma-deposited silicon nitride films, this hydrogen originates from the precursor gases used in the deposition process, and it may be bonded to nitrogen and silicon or trapped in molecular or atomic form in microvoids within the network structure.[3,4,5]

Silicon nitride is used in inversion layer solar cells,[6] thin film transistors,[7] and memory devices[8] because of its excellent dielectric properties. Particularly useful is its high dielectric permittiviy, which makes it a promising candidate to substitute silicon dioxide in the gate structure of field effect transistors. Current levels of integration in microelectronic devices demand a rigorous decrease of the gate dielectric thickness in order to keep pace with the downscaling of the transistor lateral dimensions. This trend has taken silicon dioxide to its limit of performance, where direct tunneling currents become comparable to off-state drain to source currents.[9,10] The higher dielectric constant of SiN_x:H makes possible increasing the physical thickness of the dielectric without reducing the capacitance and transconductance of the structure. In other words, a small equivalent oxide thickness is retained as needed by present technological requirements, but with a physically thicker film that avoids the limitations of a thin oxide layer.[11,12]

However, the practical realization of the above approach finds a serious limitation due to the higher stress of silicon nitride compared to silicon dioxide.[13,14] This stress originates from its higher average coordination number and results in a defective interface with the silicon substrate, which in turn causes a large density of charge-trapping defects.[15] A thorough understanding of the dielectric structure is needed in order to advance in this direction. Up to now a number of technological approaches have been tried to overcome this difficulty. Essentially, these techniques keep up silicon dioxide as the main dielectric layer, especially at the interface with the silicon wafer, and then incorporate silicon nitride to increase the thickness up to a value that eliminates tunneling currents and ion migration[16,17] or, alternatively, achieve the same effect by means of an interfacial monolayer nitrogen nitridation that avoids tunnel conduction and a top surface monomolecular layer nitridation that blocks ion migration.[18,19] This article provides some basic understanding of the network topology of SiN_x:H, which we believe will be valuable to progress in the technological applications. The study of the response of the dielectric to thermal treatments not only helps to achieve this understanding, but it is also important because of the potential benefits that controlled thermal processes may have on the bonding structure and interfacial characteristics.

Rapid thermal annealing (RTA) has proved to be a useful

tool for the postformation treatment of gate dielectrics.[20] Compared to conventional furnace annealing, it has the important advantage of careful control of the thermal budget applied to the sample, as well as of the annealing atmosphere. The early studies of rapid thermal annealing investigated the influence of RTA conditions on interface charges, interface trap distributions, and dielectric breakdown (see Ref. 20 for a review). The ambient was either nitrogen or argon, having the thermal cycle in common but differing in the low-level nitridation that takes place when using N_2. The effects of these treatments were a reduction in the flat-band voltage or in the dielectric fixed charge, and a decrease in the density of midgap interface traps, while the dielectric breakdown was found not to degrade. Most of these studies focused on silicon oxide, due to its prevailing technological importance, but latter investigations showed that similar effects were also present in silicon nitride,[21,22] although in some cases the treatments were applied by conventional annealing.[23] In addition to the improvement of the electrical properties relevant from the point of view of device performance, some studies have also been published about the structural processes taking place in the nitride lattice during the thermal process.[2,24,25,26] However, none of these previous studies had developed into detailed molecular models of the reactions pathways that can explain the strong dependence of the results on the as-grown characteristics of the dielectric, specially on its hydrogen content, and therefore on the preparation method.

The aim of this paper is to provide significant and clarifying new understanding on some aspects of the physicochemical processes that occur in silicon nitride as a function of annealing temperature. For that purpose the analysis of composition by ion beam techniques was complemented with the information on the bonding environments that can be obtained from the absorption bands in the infrared spectra. We will show that the combination of these techniques yields a set of complementary data on changes of composition and bonding that is suitable to interpret in terms of thermally activated network bond reactions that describe the rearrangement of the film microstructure during the annealing treatment at elevated temperatures. On the basis of special reaction equations we are able to estimate the relevant activation energies and to correlate them with the most important elemental processes.

II. EXPERIMENTAL PROCEDURES

Amorphous silicon nitride thin films with a variable nitrogen-to-silicon ratio and hydrogen content were deposited by a chemical vapor deposition process activated by an electron cyclotron resonance (ECR) plasma. The system consisted on an Astex 4500 reactor attached to a high-vacuum chamber that was pumped down to 2×10^{-7} mbar before each deposition run. The process pressure depended on the total gas flow and was selected to 0.67 mTorr. The ECR resonance condition was achieved by coupling a 100-W microwave to the divergent magnetic field created by a single magnet.[27,28] No deliberate heating was applied to the substrate holder. The dielectric films were grown on silicon (111) *p*-type high-resistivity ($\rho=80\,\Omega$ cm) substrates that were previously subjected to a conventional cleaning process.[29] The deposition variable that most influences the properties of the dielectrics is the precursor gas flow ratio (nitrogen to silane in this case) used in the film growth, and which we shall denote as R.[27,29] The present study will focus on three particular types of films (silicon rich, near stoichiometric, and nitrogen rich) obtained with three values of the parameter R and to be specified in Sec. III A. Each of these sample types is representative of a special bonding configuration that results in different microstructures with a characteristic response to thermal treatments. The thickness of the samples was chosen so that it produced enough absorption for adequate infrared spectra. It was 190 ± 10 nm for the silicon-rich films, 240 ± 20 nm for the near-stoichiometric series, and 300 ± 15 nm for the nitrogen-rich samples. These values were obtained with a Dektak profilometer with 5% accuracy. The higher error margin given for the near-stoichiometric series is due to a wider dispersion of values between samples deposited in different deposition runs. The thickness decreases with increasing silicon content because the higher stress introduced by the high coordination number of the silicon atoms limited the maximum thickness that could be grown without producing film peeling.

After film growth the samples were introduced in a rapid thermal annealing furnace, model Modular Processes Technology RTP-600, where they were treated at temperatures between 300 and 1050 °C during 30 s in a controlled inert gas (argon) atmosphere.

The analysis of the film composition and of the bonding structure was done by a combination of ion beam techniques, energy dispersive x-ray microanalysis (EDX) and Fourier transform infrared spectroscopy. The nitrogen-to-silicon ratio, which we shall refer to as the film stoichiometry and will be denoted as x in the formula $SiN_x:H$, was determined by Rutherford backscattering spectrometry (RBS) and averaged with the value obtained by EDX microanalysis to compensate for the systematic errors introduced by each of these techniques. The RBS spectra were measured with 1.4 MeV He^+ ions and then fitted by an iterative computer simulation program, while the EDX analysis was performed with a beam voltage of 5 kV comparing with a stoichiometric Si_3N_4 standard sample and evaluated taking into account the limited film thickness. In order to study the evolution of hydrogen in the film as a function of annealing temperature, combined use was made of heavy ion elastic recoil detection analysis (HI-ERDA) and infrared spectroscopy by the Fourier transform method. The HI-ERDA measurements were carried out at the heavy-ion accelerator facility of the Ionen-Strahl-Laboratorium of the Hahn-Meitner-Institut in Berlin. Measuring with heavy ions (120 MeV ^{86}Kr for the results presented in this study) permitted the simultaneous detection of all elements present in the sample including hydrogen.[30] The scattered ions were detected by a mass- and energy-dispersive time-of-flight system, with a solid angle of 0.4 msr, and a large scattering angle of 60° was used.[31] Although the beam current could be controlled with an accuracy of 5%, the total dose applied to each sample could deviate by up to 15% due to difficulties in determining the exact beam

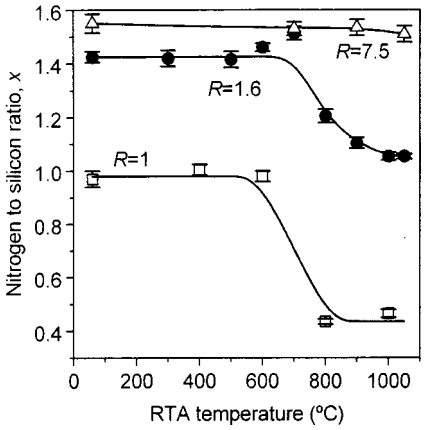

FIG. 1. Nitrogen-to-silicon ratio of the three types of films, determined by Rutherford back-scattering spectrometry and energy dispersive x-ray microanalysis and averaged to compensate for the systematic errors introduced by each of these techniques. Lines are a guide for the eye.

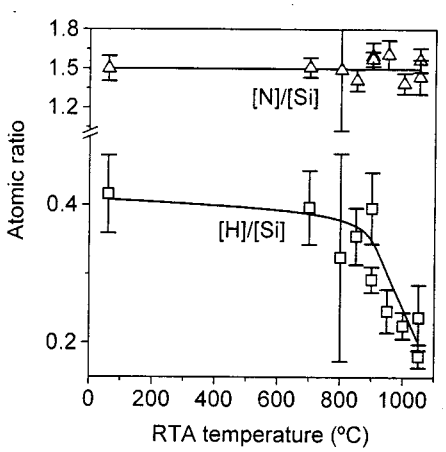

FIG. 2. Atomic ratios of nitrogen to silicon and hydrogen to silicon, determined by ERDA for several films deposited with $R=7.5$ and annealed at temperatures between 700 and 1050 °C. Lines are drawn as guides for the eye.

spot size on the sample surface. If the ion dose is not kept below $10^{12}\,\mathrm{cm}^{-2}$ then a correction procedure must be applied to compensate for the systematic errors due to beam-induced losses of hydrogen and nitrogen.[30] The data presented in the next section have been corrected for this effect. While the ERDA detects the total amount of hydrogen atoms present in the film irrespective of their chemical state, the infrared spectroscopy is only sensible to that part of hydrogen that is bonded to nitrogen or silicon producing the well-known Si-H and N-H phonon bands. The infrared spectra were recorded with a Nicolet 5PC Fourier transform spectrometer, and the density of bonded hydrogen was deduced from the area of the Si-H and N-H stretching bands applying the calibration factors obtained by Lanford and Rand.[32]

III. RESULTS

A. Composition analysis

The total atomic concentration of nitrogen and silicon present in the samples was determined by RBS and EDX and the nitrogen-to-silicon ratio x, also called stoichiometry in this work, was calculated. Figure 1 shows the average of the RBS and EDX values of this parameter obtained for each sample. Error bars represent relative uncertainties, not absolute ones, resulting from eight simulation fits in the case of RBS and the estimated standard deviation of $\pm 0.3\%$ in the case of EDX. From Fig. 1 the three types of investigated films referring to three values of the parameter R can be specified as follows: (1) silicon-rich films grown with $R=1$ having as-grown compositions of $x=0.97$, (2) near-stoichiometric films grown with $R=1.6$ and having as-grown compositions of $x=1.43$, and (3) nitrogen-rich films grown with $R=7.5$ having as-grown compositions around $x=1.55$. As the silicon-rich and near-stoichiometric series lose nitrogen above a certain annealing temperature (Fig. 1), we shall refer to each series by their value of R or their as-grown composition. In addition to silicon and nitrogen, the samples deposited with $R=7.5$ also showed a small amount of oxygen (less than 3 at %). From Fig. 1 the most important conclusion with regard to the thermally activated network bond reactions to be proposed in Sec IV is: the stoichiometry of the nitrogen-rich films ($R=7.5$) is essentially not affected by any annealing temperature in the studied range whereas the near-stoichiometric samples lose nitrogen above 700 °C and the silicon-rich films experience a similar and even more pronounced effect above 600 °C.

Hydrogen, which is also present in the films but cannot be detected by RBS and EDX, was analyzed by ERDA spot checks of the as-grown films to give a typical concentration of the order of about 10 at %. For a series of nitrogen-rich films grown with $R=7.5$ a complete RTA temperature dependence was analyzed. The results, which are shown in Fig. 2, confirm that no significant nitrogen loss occurs for these films at any annealing temperature. The nitrogen-to-silicon ratio x remains constant. On the contrary, the trend followed by the content of hydrogen indicates that this element diffuses out of the film at the annealing temperatures of the studied range, that is to say, above 700 °C.

Since for all of the samples analyzed by ERDA also the infrared spectra were recorded there was a data set available to correlate the Si-H and N-H phonon band intensities with the total hydrogen concentration and to determine the corresponding quantities of calibration. In a recent paper,[30] we have shown that these calibration parameters were in reasonably good agreement with those originally found by Lanford and Rand[32] although these authors analyzed nitride films obtained by a rather different deposition method and using nuclear reaction analysis to determine the total hydrogen concentration. For this reason, it seems to be justified to use the infrared absorption band areas as a reliable set of data representing the actual hydrogen content in our films and as a basis for the discussion of changes as a function of the annealing temperature for the three types of films specified above.

B. Bonding configuration

Three types of bonds are detected as absorption bands in the infrared spectra of silicon nitride. These are the silicon-

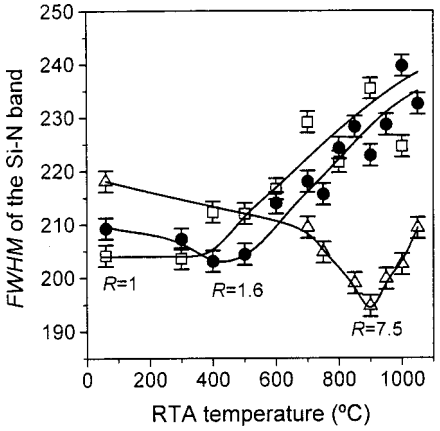

FIG. 3. Full width at half maximum of the infrared absorption band corresponding to the Si-N asymmetric stretching mode vibration. The results correspond to the three different types of films analyzed in this study and obtained with the precursor gas flow ratios indicated in the figure. Lines are guides for the eye.

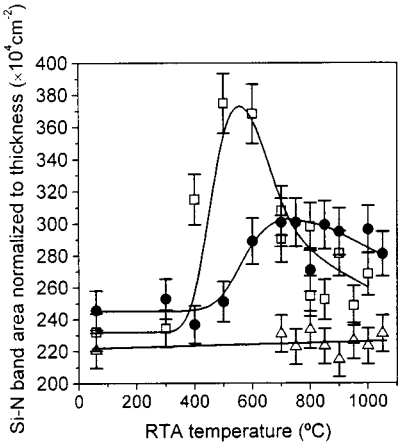

FIG. 4. Area of the Si-N band normalized to film thickness. Data for the silicon-rich films ($R=1$) are represented as □, for the quasistoichiometric series ($R=1.6$) as ●, and for the nitrogen-rich samples as △. The main source of error is introduced by the determination of the film thickness with a profilometer, which is estimated to have an accuracy of ±5%, as indicated by the error bars. Lines are drawn to guide the eye.

nitrogen, silicon-hydrogen, and nitrogen-hydrogen bonds. The silicon-silicon vibration is inactive in silicon nitride. In this section we will be concerned with the information that can be extracted from these absorption bands about the density of bonds and their chemical configuration and near-neighbor arrangements.

1. Si-N absorption band

This band is due to an asymmetric vibration of the Si-N bond. Depending on the near-neighbor environment the maximum absorption can occur for a wave number between 750 and 970 cm^{-1}.[33,34,35] Besides the dependence on the electronegativity of the surrounding atoms, the band shape is also affected by the range of bond angles, which modify the vibration frequency and therefore determine the width of the band. Thus, the FWHM (full width at half maximum) of the band reflects the overall disorder of the network topology. The higher the disorder, the higher will be the range of bond angle distortion and therefore the broader will be the absorption band. Figure 3 shows the evolution of the Si-N band FWHM as a function of annealing temperature for the three types of films. Error bars are estimated from the spectra datapoint spacing. A significant decrease is observed for the nitrogen-rich composition, and at lower annealing temperatures also for the quasistoichiometric films, indicating a thermally activated reordering of the network, with bond angles returning to their thermodynamically most stable values. On the contrary, the films with the silicon-rich composition do not experience this lattice relaxation. Above a certain temperature, that depends on the composition, the bandwidth increases indicating that some process begins to produce a structural disorder. In the discussion section we will relate this process to bond reactions involving hydrogen and nitrogen release that also are suggested by the results of composition and bonded hydrogen density.

The area of the Si-N absorption band is proportional to the density of these bonds. The calibration of this band (i.e., the determination of the oscillator strength) is not as well established in the scientific literature as it is the calibration of the Si-H and N-H bands to obtain the total content of hydrogen. Although some authors[33] have attempted a calibration of the Si-N band area, the results seem to be controversial, since the band maximum shifts with the composition indicating that the calibration constant may also depend on the chemical environment of the bond.[33,36] For this reason, in Fig. 4 we have plotted the area of this band versus annealing temperature without converting it to bond density. Nevertheless, within each composition series the plot is considered to indicate the proper trends of the bond density evolution of these films. So, for the silicon-rich ($R=1$) and quasistoichiometric ($R=1.6$) samples there is a significant increase with annealing temperature up to 600 °C in the first case and 700 °C in the second. As we will see in the discussion section, this is in agreement with a certain bond network reaction that will be considered to occur in this range of temperatures. For higher temperatures the band area decreases together with the loss of nitrogen, and as we will report in the following Figs. 5 and 6, with the loss of hydrogen.

2. Si-H and N-H absorption bands

Applying the calibration factors of Lanford and Rand,[32] we have obtained the atomic concentration of bonded hydrogen in our films, and Figs. 5 and 6 represent this quantity for the three types of films as a function of the annealing temperature. In the same way as for the data of Fig. 4, the main source of error also comes here from the determination of the film thickness. The silicon-rich ($R=1$) and near-stoichiometric ($R=1.6$) compositions exhibit both Si-H and N-H bonds, while for nitrogen-rich films only N-H bonds are found. In as-grown films, an additional amount of hydrogen in atomic or molecular form is suspected that probably is trapped in microvoids of the structure formed during the growth process. This might explain that at moderate anneal-

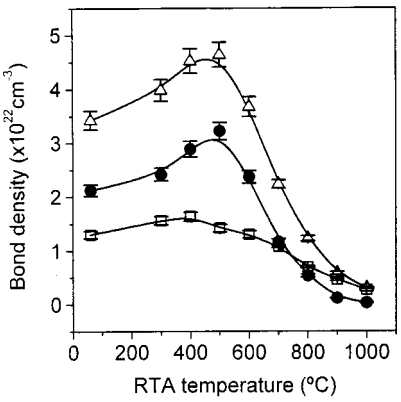

FIG. 5. In the silicon-rich ($R=1$) films, Si-H bonds (●) predominate over N-H bonds (□). The total content of bonded hydrogen is denoted as △. Lines are drawn as guides to the eye.

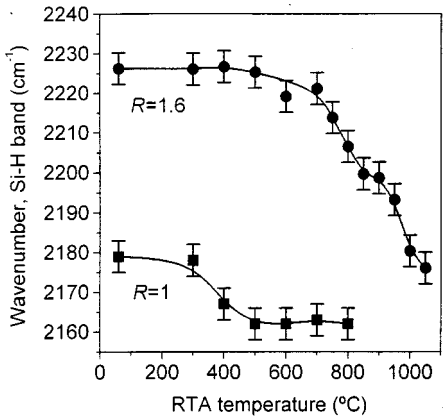

FIG. 7. Peak absorption wave number of the Si-H stretching mode for those two types of films that present this band in the infrared spectra. Lines are drawn as guides to the eye.

ing temperatures new hydrogen bonds with nitrogen or silicon are formed and thus the density of bonded hydrogen increases in this temperature range. For higher annealing temperatures hydrogen is lost due to the breaking of Si-H and N-H bonds. In the next section we will propose a reaction model for these processes.

The wave number, at which the maximum absorption takes place, contains information about the near-neighbor arrangements around the vibrating bond. The higher the electronegativity of the surrounding atoms, the higher is the frequency (or wave number) of the vibration. The positions of the peak absorption of the Si-H stretching mode are shown in Fig. 7 for the silicon-rich and near-stoichiometric samples, and those of the N-H bands for the nitrogen-rich and near-stoichiometric films in Fig. 8. The silicon-hydrogen band shifts to lower wave numbers as the annealing temperature increases. For the samples deposited with $R=1.6$ this shift occurs above 700 °C, in perfect coincidence with the onset of nitrogen and hydrogen loss whose details we will study in the next section. For the silicon-rich samples, the shift takes place already between 300 and 500 °C that it is not related to the same process as for the near-stoichiometric composition. Instead it must be associated with the processes that take place at lower annealing temperatures, causing an incorporation of bonded hydrogen and a chemical ordering reaction being responsible for a decrease of the nitrogen-hydrogen bond density at a lower temperature than in the case of the Si-H bonds. As shown in Fig. 8, the peak shift of the N-H band is in the opposite direction, toward higher wave numbers, and only takes place in the nitrogen-rich series, in contrast to the unchanged N-H band position in the near-stoichiometric samples. The observed frequency increase of the N-H vibration for the nitrogen-rich films can be interpreted to originate from an increase of the electronegativity of the nearest neighbors as a consequence of the process of hydrogen release in these films. In the next section we will introduce and discuss simple reaction models that are suitable to describe consistently all observed features concerning the dependence of bonding configuration and composition of our films on the annealing temperature at the RTA process.

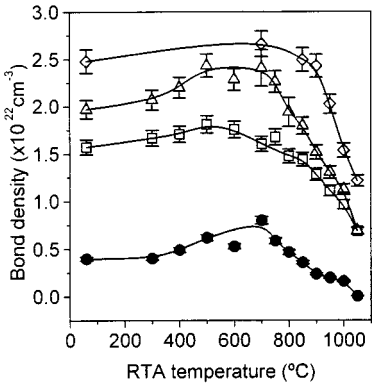

FIG. 6. Density of bonded hydrogen for the quasistoichiometric ($R=1.6$) and nitrogen-rich ($R=7.5$) samples. The films deposited with $R=1.6$ have both N-H (□) and Si-H (●) bonds, while the $R=7.5$ films only show N-H bonds (◇) and their density is larger than the total amount of bonded hydrogen for the $R=1.6$ case (△). Lines are guides to the eye.

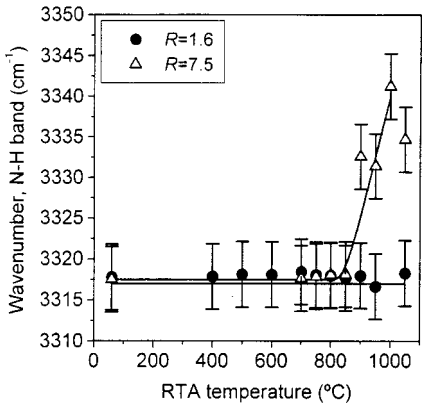

FIG. 8. Wave number of the maximum of the N-H absorption band vs annealing temperature for the near-stoichiometric and nitrogen-rich compositions. Only the latter one shows a shift of this band and it occurs at the highest annealing temperatures, those that cause the loss of bonded hydrogen. Lines are a guide to the eyes.

IV. DISCUSSION

1. Network relaxation

We begin the discussion of the results by stressing the striking difference between the silicon-rich samples and the other two types of films with respect to the temperature dependence of the Si-N bandwidth (see Fig. 3). While the nitrogen-rich and near-stoichiometric samples experience an initial decrease of the FWHM parameter, up to an intermediate annealing temperature (900 °C in the first case and 400–500 °C in the second), the silicon-rich films do not show this behavior. The decrease of the FWHM parameter points to a thermal relaxation process whereby the distorted bond angles being present in the as-grown film network return to a stable minimum-energy configuration approaching their thermal equilibrium values. The absence of an equivalent relaxation process for the silicon-rich case is attributed to a higher stress due to the higher coordination number of silicon (4) with respect to nitrogen (3).[37] It is known that a percolation threshold exists in silicon nitride at a composition of about $x=1.1$.[38] For nitrogen-to-silicon ratios below this value, i.e., also for our silicon-rich film series ($R=1$ and as-grown stoichiometry $x=0.97$), there are continuous chains of Si-Si bonds extending throughout the whole lattice. These chains increase the connectivity of the network and make the structure very rigid and stressed because of the high coordination number of silicon. This explains why the network of these films does not experience a measurable thermal relaxation process. For the other two types of films, the as-grown composition is above the percolation threshold ($x=1.43$ for $R=1.6$ and $x=1.55$ for $R=7.5$) and therefore uninterrupted percolation chains do not exist. The network of these films has more flexibility because of the lower number of constraints present,[39,40,41] and therefore a thermally activated relaxation process may become active.

This interpretation of the Si-N bandwidth changes is in complete accordance with the results of a previous publication dealing with the analysis of the optical absorption edge of our films in the visible region.[37] In an amorphous solid the slope of this edge is indicative of the degree of order/disorder because it is affected by the presence of defect-generated band tails. The results presented in Ref. 37 for samples obtained under the same deposition conditions as those analyzed in this study confirm the thermal reordering of the film structure for temperatures below those ones that promote the release of hydrogen, except for the silicon-rich films whose behavior reveals again a rigid and strained structure.

2. Hydrogen redistribution at moderate annealing temperatures

In order to explain thermally induced changes of the bonded hydrogen content deduced by infrared spectroscopy and of the nitrogen-to-silicon ratio in the films obtained by RBS/EDX measurements, we will propose a set of network bond reactions that are supported by the experimental evidence presented in the previous section. Beginning with the range of moderate annealing temperatures, we observe that below 600 °C for the silicon-rich composition and 700 °C for the near-stoichiometric films, the nitrogen-to-silicon ratio remains constant (Fig. 1) while the content of bonded hydrogen increases, in a more noticeable way in Si-H bonds than in the N-H, and the latter ones begin to decrease at a lower temperature than the former. We interpret these results as an evidence for the following chemical ordering reaction:

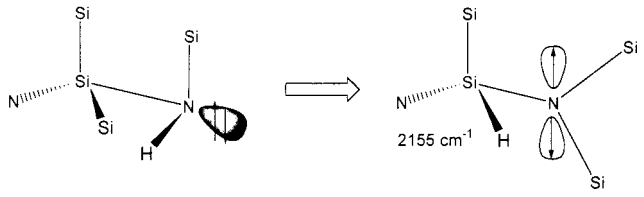

FIG. 9. Schematic illustration of the trend for chemical order whereby at moderate temperatures the Si-H and Si-N bonds are favored at the expense of the Si-Si and N-H ones, as predicted by the free-energy model of Yin and Smith. In a chemical environment such as the one of this figure, the increase of the Si-H bond density explains the shift of the maximum of this band toward the value characteristic of the Si-H vibration in a silicon-rich setting.

$$\text{Si-Si}+\text{N-H}\rightarrow\text{Si-H}+\text{Si-N}. \tag{1}$$

This is a well-known[42] network bond process favored by the tendency to approach chemical equipartition, whereby the formation of Si-H and Si-N bonds is favored at the expense of Si-Si and N-H bonds. Taking into account nominal bond energies[43,44] this process is exothermic, with a favorable energy balance of 0.25 eV. The formation of Si-N bonds also justifies the increase of the Si-N absorption band area observed in Fig. 4. In the nitrogen-rich films this process does not take place because of the much lower density of Si-Si bonds, and therefore the Si-N band area remains unaffected by the annealing temperature and no Si-H band appears in the spectrum.

The bond scheme drawn in Fig. 9 might illustrate how reaction (1) proceeds in a silicon-rich environment corresponding to the $R=1$ series. The new Si-H bond being formed in this process has two nitrogen and one silicon atoms as near neighbors. In this environment its vibration frequency is 2155 cm^{-1}.[33,35,45,46] The formation of new Si-H groups in this configuration causes the corresponding absorption band to shift toward this value in the silicon-rich series (see Fig. 7). The as-grown position of the absorption band, centered around 2180 cm^{-1}, indicates that the predominant configuration of the nonannealed samples is H_2SiN_2.[33,35,45,46] The new $HSiN_2Si$ groups (or possibly also H_2SiNSi, depending on the initial configuration) that result in reaction (1), with vibration frequency in 2155 (or 2140 cm^{-1}, respectively) then shift the peak position to an intermediate value. Another point of interest in the bonding diagram of Fig. 9 is the nitrogen atom electronic orbital hybridization. In the initial situation it is bonded to two silicon atoms and one hydrogen atom, and the most stable configuration is the sp^3 tetrahedral hybridization.[47,48] In the final situation the nitrogen will be bonded to three silicon atoms, as a consequence of the bond interchange reaction. In this case the interaction between the doubly occupied p_z nonbonding orbital perpendicular to the bond plane and the internal type *d* orbitals of

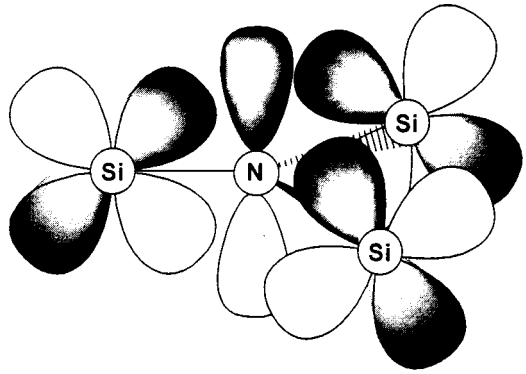

FIG. 10. Schematic illustration of the p_π-d_π interaction between the nitrogen nonbonding orbital and the internal type *d* orbitals of the three silicon atoms that it has as nearest neighbors. This form of bonding of the nitrogen atom is unique of the N-Si_3 and N-Ge_3 cases.

the three silicon atoms now makes the sp^2 planar hybridization of the nitrogen atom highly stable.[47,49] This interaction has been schematically pictured in the orbital diagram of Fig. 10.

3. Hydrogen release at high annealing temperatures

Turning now to the high-temperature range, we note first that the silicon-rich ($R=1$) and near-stoichiometric ($R=1.6$) samples experience a loss of nitrogen for temperatures higher than 600 °C in the first case and 700 °C in the second (see Fig. 1). The process of nitrogen release is accompanied by loss of bonded hydrogen (see Figs. 5 and 6). This does not occur for the nitrogen-rich ($R=7.5$) composition where a constant nitrogen-to-silicon ratio is maintained (Figs. 1 and 2). In the nitrogen-rich sample series the loss of bonded hydrogen occurs mainly above 900 °C (Fig. 6) although the total hydrogen density decreases from about 700 °C (Fig. 2) indicating that nonbonded hydrogen trapped in microvoids starts to leave the sample at that temperature.

We now attempt to describe the process of nitrogen and hydrogen release for the $R=1$ and $R=1.6$ samples by a reaction that involves cooperative interaction between Si-H and N-H bonds and the effusion of an ammonia fragment that is able to capture rapidly an additional hydrogen atom and to form an ammonia molecule:

$$\text{Si-H}+\text{H-NSi-H}\rightarrow\text{Si-Si}+\text{NH}_3\uparrow. \tag{2}$$

Figure 11 illustrates this process with a bond diagram of the intervening groups. The nitrogen atom has a tetrahedral sp^3 configuration that facilitates the formation of a H-bonding interaction in which the strong negative charge density of a doubly occupied sp^3 nonbonding orbital attracts a nearby hydrogen atom of a Si-H bond. The bond strength, thus, is weakened, splitting off and subsequent capture of the hydrogen atom by the nitrogen atom is favored and, finally, the resulting ammonia fragment will be released.[26,50] The energy balance of this process is exothermic if it is assumed that the nitrogen atom is originally bonded to only one silicon atom. In that case a favorable energy output of 0.15 eV can be estimated for Eq. (2). The vibration frequency of the remaining Si-H bond is affected by the change of electronegativity that involves the formation of the new Si-Si weak bond between the two silicon dangling bonds produced in this process. As a consequence the oscillation wave number shifts to a lower value, from 2220 cm^{-1} in the original configuration ($HSiN_3$) to 2155 cm^{-1} in the final situation ($HSiN_2Si$), in accordance with the lower electron affinity of the new environment.[33,35,45,46] This is in agreement with the experimentally observed peak shift for the $R=1.6$ case (see Fig. 7).

In the $R=1$ films the peak shift has not been detected in that range of temperatures relevant for reaction (2). In these samples the Si-H bonds are located in silicon-rich environments such as the H_2SiNSi (2140 cm^{-1}) and $HSiN_2Si$ (2155 cm^{-1}) groups—produced as discussed in Sec. IV 2 by reaction (1)—and the H_2SiN_2 (2175 cm^{-1}) groups present in the as-grown samples. When the two Si-H bonds that take part in the process of Fig. 11 and Eq. (2) are in the form of H_2SiN_2

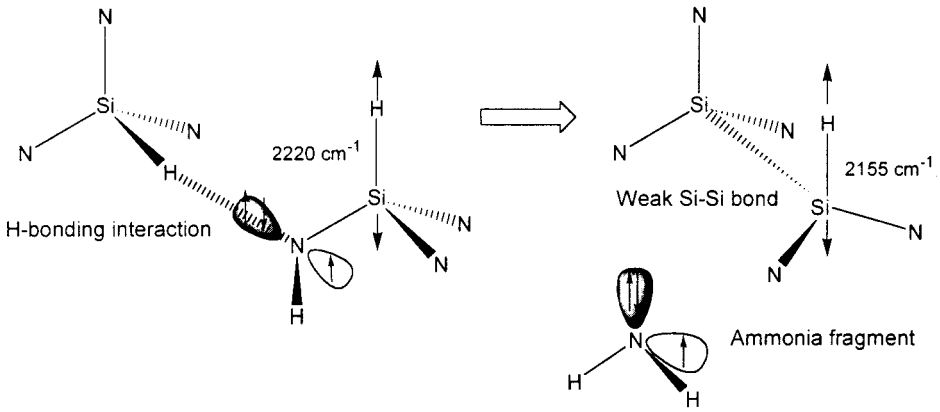

FIG. 11. Schematic representation of reaction (2) for the particular case of the films of the $R=1.6$ series, showing the Si-H stretching vibrational modes and their respective frequencies. The doubly occupied nitrogen orbital is represented in dark color with two arrows of opposite sense that indicate two electrons of opposite spin. The clear orbital indicate a dangling bond, which if it were bonded to silicon would increase the energetic barrier of the process, as it probably occurs in the nitrogen-rich samples preventing the loss of nitrogen.

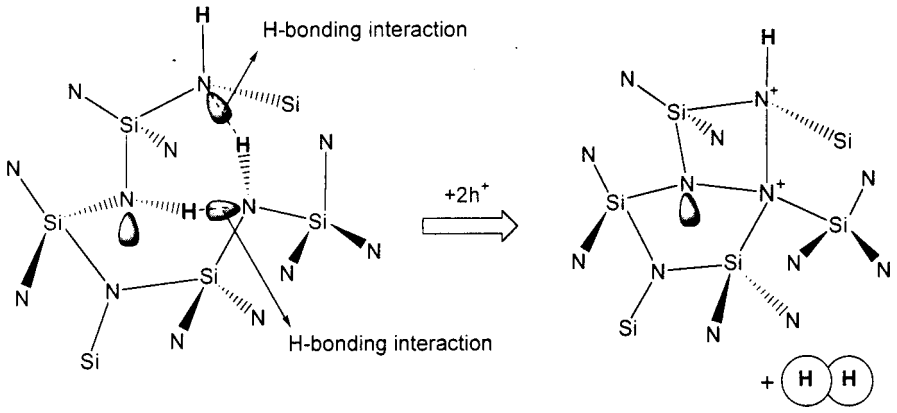

FIG. 12. Scheme of a possible environment for the effusion of molecular hydrogen from near N-H groups weakened by the H-bonding interaction. The process takes place with the simultaneous capture of one hole for each hydrogen atom released, so that the broken bonds are reconstructed with the formation of weak N-N bonds that contribute to compensate the unfavorable energy balance of the reaction. As a result, the nitrogen atoms that have participated in the process remain in a positively charged tetracoordinated configuration.

groups the resulting Si-H bonds that remain in the nitride will be of the $HSiN_2Si$ and H_2SiNSi types but, as these groups were already predominating as a consequence of the bond interchange reaction taking place at a lower temperature (Fig. 9), a peak shift cannot be observed (Fig. 7; silicon-rich $R=1$ samples). If, on the other hand, the groups that interact in the form of Fig. 11 are the $HSiN_2Si$ and H_2SiNSi then the only reaction product that contains the Si-H bond is of the type $HSiNSi_2$, whose oscillation frequency would be at 2080 cm^{-1}. But these Si-H bonds are located in environments that are very silicon rich, are much weaker, and easily decompose into H_2 and new Si-Si bonds as it is known from amorphous silicon.[51]

The process of hydrogen release in the nitrogen-rich film ($R=7.5$) follows a different mechanism. These samples do not exhibit any detectable loss of nitrogen in the whole range of annealing temperatures. Therefore the process of hydrogen outdiffusion cannot take place with a simultaneous release of nitrogen as described above. Since there are no detectable Si-H bonds, the process can only involve N-H bonds. As a straightforward reaction to describe such process we consider

$$\text{Si-N-H}+\text{Si-N-H}\rightarrow 2(\text{Si-N}\cdot)+\text{H}_2\uparrow. \tag{3}$$

As with the silicon-rich and near-stoichiometric cases, the process also takes place with the formation of H-bonding interactions, in this case between doubly occupied hybrid sp^3 nitrogen orbitals and hydrogen atoms of a N-H group in the next vicinity. This interaction weakens the N-H bonds and makes possible that it splits up, freeing the hydrogen atom. If this has a chance to encounter a second hydrogen atom it will form a hydrogen molecule and escape from the film. Figure 12 depicts this process in the nitrogen-rich environment of the $R=7.5$ films. In this figure the dangling nitrogen bonds that result from the broken N-H bonds are healed by the formation of weak N-N bonds. This is concluded from two arguments. First, since the energy balance of equation (3) is highly endothermic (-3.62 eV) due to the strong bonding energy of the N-H bonds[43,44] it is necessary to integrate an additional mechanism of energy gain in order to arrive at the reduced value of the activation energy of the process of hydrogen release, which as we will see in the last part of this section is 2 eV. Second, the increase of the vibration frequency of the N-H bonds that remain in the network when part of the hydrogen is released (see Fig. 8) indicates an increase of the average electron affinity of the environment, which fits well with the formation of N-N bonds if one of these nitrogen atoms is also bonded to one of the remaining hydrogen atoms, as shown in Fig. 12.

4. Activation energies

We will finish now the discussion of the thermally activated microstructural processes in silicon nitride by estimating some activation energies from the experimental data of hydrogen outdiffusion. Assuming that the reactions of hydrogen release [Eqs. (2) and (3)] obey a chemical kinetics of second order we find that the desorption rate of the bonded hydrogen is given by

$$-\frac{d[C(\text{H})]}{dt}=-\frac{d([\text{N-H}]+[\text{Si-H}])}{dt}=2K_1[\text{N-H}][\text{Si-H}] \tag{4}$$

in the first case [corresponding to Eq. (2)], and

$$-\frac{d[C(\text{H})]}{dt}=-\frac{d[\text{N-H}]}{dt}=2K_2[\text{N-H}]^2 \tag{5}$$

in the second [corresponding to Eq. (3)], where [N-H] and [Si-H] are the densities of N-H and Si-H bonds, respectively, and $[C(\text{H})]$ is the total concentration of bonded hydrogen. The kinematic reaction constants, K_1 and K_2,[25,52] depend on temperature through an Arrhenius-type law in which the activation energy (E_a) appears in the exponent and the process entropy (ΔS^*) in the preexponential factor. To study the influence of the temperature it is necessary to integrate Eqs. (4) and (5) between an initial and a final time, which in our

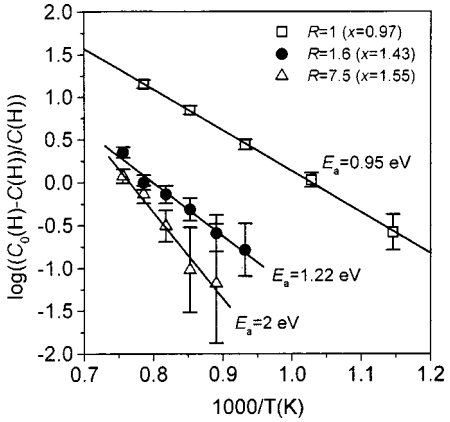

FIG. 13. Arrhenius plot of the decrease of bonded hydrogen vs the inverse of the temperature for the three types of films. The solid lines are fits to Eq. (6), from which the activation energy of the process is calculated and indicated in this figure for each sample series. Error bars are calculated from the respective error of the hydrogen concentration in Figs. 5 and 6.

study is given by the constant duration of RTA that amounted to 30 s. Performing the integration leads to the expression

$$\frac{C_0(\mathrm{H})-C_t(\mathrm{H})}{C_t(\mathrm{H})}=C_0(\mathrm{H})\times t\times A\, e^{\Delta S^*/R}e^{-\varepsilon_a/RT}, \qquad (6)$$

where t is the time interval, T is the temperature of the annealing process, R is the molar gas constant, A is a proportionality factor implicit in the kinematic constant, and $C_0(\mathrm{H})$ and $C_t(\mathrm{H})$ are the initial and final hydrogen concentrations, respectively, which contain the bond densities that appear in Eqs. (4) and (5).[26] Since the left part of Eq. (6) can be obtained from the experiment an Arrhenius plot of this quantity will provide the sum activation energy of the process chain regulating the measured hydrogen release. Figure 13 shows that in fact the hydrogen release of all three types of samples is well described by the thermal activation law of equation (6). Two activation energies are fairly close to each other: $E_a=(0.950\pm0.016)$ eV for the silicon-rich ($R=1$) films and $E_a=(1.22\pm0.09)$ in the near-stoichiometric ($R=1.6$) case. The films with the larger nitrogen content ($R=7.5$), in contrast, have a significantly higher value of the activation energy, $E_a=(2.00\pm0.19)$ eV.

These results concerning the activation energy are consistent with the mechanisms presented above explaining the release of hydrogen. In the silicon-rich and near-stoichiometric samples the process of hydrogen loss takes place through the same mechanism, which is exothermic and therefore does not put a condition on the activation energy. Accordingly, the activation energy is very similar in both cases. There is, nevertheless, a difference in the range of temperature in which the process takes place (from 500 °C for $R=1$ and from 700 °C for $R=1.6$). One would expect that if the process is the same, it would take the same thermal energy to initiate it and therefore the same temperature. However, there are several reasons why this is not the case here. First, one has to note that the process entropy appears in the preexponential factor of the Arrhenius law, and that although it cannot affect the slope of the fit of Fig. 13 it can affect the zero ordinate, that is to say, it can shift the data vertically. On the other hand, it has to be noted as well that due to the above-mentioned similarities between the samples of the $R=1$ series and the amorphous silicon with regard to the presence of chains and clusters of Si-Si bonds and the predominance of Si-H bonds, the possibility of another process of hydrogen loss consisting on the interaction of two Si-H bonds to produce the effusion of molecular hydrogen and a weak Si-Si bond must be taken into account:

$$\mathrm{Si\text{-}H+Si\text{-}H\rightarrow Si\text{-}Si+H_2}. \qquad (7)$$

This reaction is exothermic (+0.14 eV) and therefore does not condition the value of the activation energy. It also explains that the density of Si-H bonds in the silicon-rich ($R=1$) films decreases above 500 °C, which is a temperature lower than the one that causes the loss of nitrogen described by the process of Eq. (2) and Fig. 11. This is supported by previous results of optical properties (Ref. 37) that showed that these films experienced a decrease of the band gap (consistent with the formation of Si-Si bonds) at lower temperatures than 600 °C in which the reaction given by Eq. (2) is started. In this way, the process of hydrogen release given by Eq. (7) would explain the different temperature observed for the onset of hydrogen loss between the silicon-rich and near-stoichiometric films, and would also be consistent with the slightly lower activation energy for $R=1$ (0.95 eV) in comparison with the $R=1.6$ case (1.22 eV).

The value of the activation energy for the nitrogen-rich films (2 eV) is significantly larger than for the other two types of samples. Nevertheless, it is still much lower than the N-H bond energy (4.05 eV), even taking into account the formation of a hydrogen molecule (H_2) when the effusion of hydrogen takes place in two near N-H groups, as it was proposed in process 3 (which has an endothermic energy balance of 3.62 eV). Therefore an additional mechanism of energy gain, which was proposed in Fig. 12 as the formation of a N-N bond between broken nitrogen dangling bonds, seems to be necessary. The formation of one of these bonds would reduced the net energy balance of the reaction to 1.92 eV, which is very close to the measured activation energy.

V. CONCLUSIONS

The combination of analytical techniques for the determination of the composition (combined RBS/EDX and ERDA) together with infrared spectroscopy has made it possible to study simultaneously the atomic concentrations of all elements present in amorphous hydrogenated silicon nitride dielectrics and their bonding configurations as a function of annealing temperatures. Three different types of films were obtained that have shown different behaviors in the annealing processes, depending on the way in which hydrogen is bonded. In the samples with a silicon-rich or near-stoichiometric composition, both Si-H and N-H bonds can be detected in the infrared spectra and these films experience network bond reactions characterized by the interactions between these two types of bonds. In the lower range of an-

nealing temperatures (below 600 °C for the silicon rich and 700 °C for the near stoichiometric) these dielectrics experience an interchange bond reaction favored by the tendency for chemical order whereby Si-H and Si-N bonds are favored at the expense of N-H and Si-Si bonds. At higher annealing temperatures a loss of nitrogen is detected that is explained together with the effusion of hydrogen by the formation of ammonia fragments that result from the H-bonding interaction between Si-H bonds and nearby doubly occupied nitrogen hybrid orbitals.

In the nitrogen-rich films the absence of any detectable amount of Si-H bonds prevents the above reactions from taking place. In this case no loss of nitrogen is detected at any annealing temperature. Although the ERDA measurements detect that the total content of hydrogen decreases starting at about 700 °C, the loss of bonded hydrogen takes place mainly above 900 °C. Between 600 and 900 °C the hydrogen that diffuses out of the film comes from the nonbonded atomic and molecular hydrogen trapped in microvoids of the structure. The breaking of the N-H bonds takes place with the formation of molecular hydrogen and N-N bond healing.

ACKNOWLEDGMENTS

We wish to thank the financial support of the Spanish National Office for Science and Technology under grant TIC98/0740 and the technical assistance received from the ion implantation facility ''CAI—Implantación Iónica'' of the University of Madrid. Dr. E. Martínez from the Department of Chemistry of the University of Murcia is thanked for valuable comments and suggestions.

[1] C. G. Van de Walle, in *Hydrogen in Semiconductors*, edited by C. G. Van de Walle Semiconductors and Semimetals (Academic, San Diego, 1991), Vol. 34.
[2] Z. Lu, S. S. He, Y. Ma, and G. Lucovsky, J. Non-Cryst. Solids **187**, 340 (1995).
[3] R. E. Norberg, D. J. Leopold, and P. A. Fedders, J. Non-Cryst. Solids **227–230**, 124 (1998).
[4] H. J. Stein, V. A. Wells, and R. E. Hampy, J. Electrochem. Soc. **126**, 1750 (1979).
[5] H. J. Stein, S. M. Myers, and D. M. Follstaedt, J. Appl. Phys. **73**, 2755 (1993).
[6] A. Beyer, G. Ebest, and R. Reich, Appl. Phys. Lett. **68**, 508 (1996).
[7] T. P. Ma, IEEE Trans. Electron Devices **45**, 680 (1998).
[8] D. Xu and V. J. Kapoor, J. Appl. Phys. **70**, 1570 (1991).
[9] H. Y. Yang, H. Niimi, and G. Lucovsky, J. Appl. Phys. **83**, 2327 (1998).
[10] H. Y. Yang, H. Niimi, J. W. Keister, G. Lucovsky, and J. E. Rowe, IEEE Electron Device Lett. **21**, 76 (2000).
[11] Y. Wu and G. Lucovsky, IEEE Electron Device Lett. **19**, 367 (1998).
[12] Y. Wu, Y. Lee, and G. Lucovsky, IEEE Electron Device Lett. **21**, 116 (2000).
[13] S. Hasegawa, Y. Amano, T. Inokuma, and e. Y. Kurata, J. Appl. Phys. **72**, 5676 (1992).
[14] M. Maeda and K. Ikeda, J. Appl. Phys. **83**, 3865 (1998).
[15] G. Lucovsky, Y. Wu, H. Niimi, V. Misra, and J. C. Phillips, Appl. Phys. Lett. **74**, 2005 (1999).
[16] Y. Ma, T. Yasuda, and G. Lucovsky, Appl. Phys. Lett. **64**, 2226 (1994).
[17] C. G. Parker, G. Lucovsky, and J. R. Hauser, IEEE Electron Device Lett. **19**, 106 (1998).
[18] G. Lucovsky, J. Vac. Sci. Technol. B **17**, 1340 (1999).
[19] H. Niimi and G. Lucovsky, J. Vac. Sci. Technol. B **17**, 2610 (1999).
[20] H. Z. Massoud, in *Rapid Thermal Annealing Processing: Science and Technology*, edited by R. B. Fair (Academic, Boston, 1993), p. 58.
[21] D. G. Park, Z. Cherr, D. M. Diatezua, Z. Wang, A. Rockett, H. Morkoç, and S. A. Alterovitz, Appl. Phys. Lett. **70**, 1263 (1997).
[22] Y. Ma, T. Yasuda, and G. Lucovsky, J. Vac. Sci. Technol. B **11**, 952 (1993).
[23] M. C. Hugon, F. Delmotte, B. Agius, and J. L. Courant, J. Vac. Sci. Technol. A **15**, 3143 (1997).
[24] L. Cai, A. Rohatgi, D. Yang, and M. A. El-Sayed, J. Appl. Phys. **80**, 5384 (1996).
[25] R. C. Budhani, R. F. Bunshah, and P. A. Flinn, Appl. Phys. Lett. **52**, 284 (1988).
[26] Z. Lu, P. Santos-Filho, G. Stevens, M. J. Williams, and G. Lucovsky, J. Vac. Sci. Technol. A **13**, 607 (1995).
[27] S. García, J. M. Martín, M. Fernández, I. Mártil, and G. González-Díaz, Philos. Mag. B **73**, 487 (1996).
[28] S. Garcia, J. M. Martín, I. Mártil, M. Fernández, I. Iborra, and G. González-Díaz, J. Non-Cryst. Solids **187**, 329 (1995).
[29] F. L. Martínez, I. Mártil, G. González-Díaz, B. Selle, and I. Sieber, J. Non-Cryst. Solids **227–230**, 523 (1998).
[30] W. Bohne, W. Fuhs, J. Röhrich, B. Selle, G. González-Díaz, I. Mártil, F. L. Martínez, and A. del Prado, Surf. Interface Anal. **30**, 534 (2000).
[31] W. Bohne, J. Röhrich, and G. Röschert, Nucl. Instrum. Methods Phys. Res. B **136–138**, 633 (1998).
[32] W. A. Lanford and M. J. Rand, J. Appl. Phys. **49**, 2473 (1978).
[33] E. Bustarret, M. Bensuoda, M. C. Habrad, J. C. Bruyère, S. Poulin, and S. C. Gujrathi, Phys. Rev. B **38**, 8171 (1988).
[34] S. Hasegawa, H. Anbutsu, and e. Y. Kurata, Philos. Mag. B **59**, 365 (1989).
[35] G. Lucovsky, J. Yang, S. S. Chao, J. E. Tyler, and W. Czubatyj, Phys. Rev. B **28**, 3234 (1983).
[36] C. Savall, J. C. Bruyère, and J. P. Stoquert, Thin Solid Films **260**, 174 (1995).
[37] F. L. Martinez, A. del Prado, I. Mártil, G. González-Díaz, B. Selle, and I. Sieber, J. Appl. Phys. **86**, 2055 (1999).
[38] J. Robertson, Philos. Mag. B **69**, 307 (1994).
[39] G. Lucovsky and J. C. Phillips, J. Non-Cryst. Solids **227–230**, 1221 (1998).
[40] J. C. Phillips, J. Non-Cryst. Solids **34**, 153 (1979); **47**, 203 (1983).
[41] H. He and M. F. Thorpe, Phys. Rev. Lett. **54**, 2107 (1985).

[42] Z. Yin and F. W. Smith, Phys. Rev. B **43**, 4507 (1991).
[43] I. N. Levine, *Fisicoquímica* (McGraw-Hill, Madrid, 1991).
[44] F. W. Smith and Z. Yin, J. Non-Cryst. Solids **137–138**, 871 (1991).
[45] B. Abeles, L. Yang, P. D. Persons, H. S. Stasiswski, and W. Lanford, Appl. Phys. Lett. **48**, 168 (1986).
[46] G. Lucovsky, R. J. Nemanich, and J. C. Knights, Phys. Rev. B **19**, 2064 (1979).
[47] G. Lucovsky, Z. Jing, and D. R. Lee, J. Vac. Sci. Technol. B **14**, 2832 (1996).
[48] Z. Jing, G. Lucovsky, and J. L. Whitten, J. Vac. Sci. Technol. B **13**, 1613 (1995).
[49] N. N. Greenwood and A. Earnshaw, *Chemistry of the Elements* (Pergamon, Oxford, 1984).
[50] Z. Lu, S. S. He, Y. Ma, and G. Lucovsky, J. Non-Cryst. Solids **187**, 340 (1995).
[51] K. Zellama, L. Chahed, P. Sládek, M. L. Thèye, J. H. von Bardeleben, and P. Roca i Cabarrocas, Phys. Rev. B **53**, 3804 (1996).
[52] Y. L. Khait, R. Weil, R. Beserman, W. Beyer, and H. Wagner, Phys. Rev. B **42**, 9000 (1990).